Powder Technology, 11 (1975) 59–67

Shearing Behaviour of Slightly Compressed Cohesive Granular Materials*

JÖRG SCHWEDES

Bayer AG, Leverkusen (Germany)

(Received June 18, 1974)

SUMMARY

In order to describe the failure properties of slightly compressed cohesive granular materials, the yield criteria must be known. Yield criteria from plasticity theory and soil mechanics are discussed with respect to their applicability to granular materials in powder technology. Shear tests are used to measure the failure properties. The shear behaviour in the flow factor tester of Jenike and in a modified version of the simple shear apparatus of Roscoe will be described. Test results from measurements with both apparatuses will be compared and it will be shown how the different results influence the design of hoppers.

INTRODUCTION

In soil mechanics the deformation of granular material should lie within elastic limits so that failure cannot occur. In contrast to this, in powder technology for most cases the state of failure must be achieved. Granular materials should flow smoothly in bins and hoppers. Stable arches or dead zones should be avoided. In order that an element of granular material begins to yield, the state of stress must become critical, *i.e.* a yield criterion must be satisfied. To determine this criterion we have to look at the granular material as a continuum. The element of material considered should be homogeneous with respect to bulk density ρ_s and the particle size should be negligible compared with the size of the element considered.

YIELD CRITERION; YIELD SURFACES

In the simple case of deformation caused by uniaxial tension or compression, the yield-point is reached if the applied stress σ equals a critical value k. We can define the following yield criterion:

$$\sigma = k \text{ or}$$

$$\sigma - k = 0$$

or for the general case

$$f(\sigma, k) = 0$$

If we consider a tridimensional deformation instead of the uniaxial one, the stress σ has to be replaced by the stress tensor with its 9 components σ_{ij}. The yield criterion for this case is

$$f(\sigma_{ij}, k) = 0$$

or if the three principal stresses σ_1, σ_2, σ_3 are known,

$$f(\sigma_1, \sigma_2, \sigma_3, k) = 0$$

It is possible to represent relations of this type graphically in a tridimensional abstract principal stress space with the three principal stresses σ_1, σ_2 and σ_3 as coordinates and the bulk density ρ_s as parameter. The resulting geometrical figures are called yield surfaces.

The yield surfaces of Tresca and von Mises are known from plasticity theory for metals [1]. In soil mechanics, using the yield criterion of Coulomb, a yield surface can be derived called the Mohr - Coulomb yield surface. This criterion, however, is not applicable to granular materials in powder technology, and indeed in soil mechanics wrong interpretations are possible. Amongst others, the experimental and theoretical investigations of Roscoe [3 - 12] in soil mechanics and of Jenike [13 - 16] in

---

* This paper was presented as a review lecture at the Symposium on "Characterization of the bulk properties of granular materials and powders" in London, Sept. 1973.

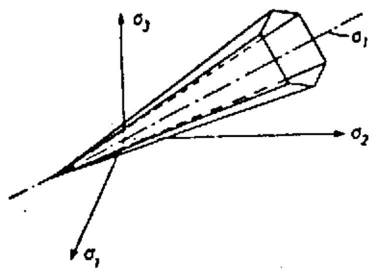

Fig. 1. Mohr - Coulomb yield surface.

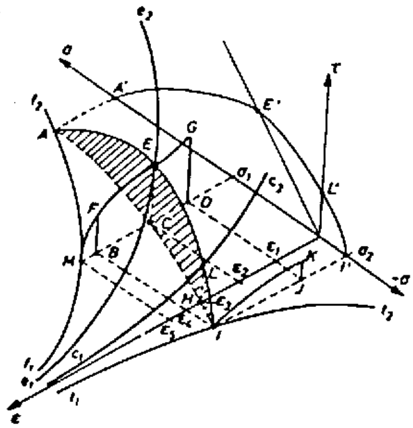

Fig. 2. Condition-diagram of Roscoe.

powder technology must be mentioned. It is beyond the scope of this contribution to explain and compare in detail the different yield surfaces, especially since the general representation in the abstract principal stress space is less convenient for practical purposes. Before reporting on this, the importance of yield surfaces is explained with the aid of the Mohr - Coulomb yield surface in Fig. 1. The properties of the surface are:

(1) States of stress, represented by the three principal stresses σ_1, σ_2 and σ_3, cause only elastic and reversible deformation if the state point $(\sigma_1, \sigma_2, \sigma_3)$ is within the yield surface.

(2) A plastic irreversible deformation takes place if the state point lies on the yield surface, and

(3) States of stress beyond the yield surface are not physically possible.

For the low compressive stresses which are of most interest in powder technology it is hard to measure principal stresses directly. Hence it is necessary to run shear tests and convert the resulting shear and compressive stresses into principal stresses in order to get yield surfaces in principal stress space. For this many experiments are necessary, so that this general representation is not very convenient for practical purposes.

CONDITION-DIAGRAM OF ROSCOE

The use of a tridimensional condition-diagram due to Roscoe (Fig. 2) overcomes this problem. The coordinates of this diagram are the shear stress τ and the compressive stress σ acting on a sample of granular material in a shear test. The third coordinate is the bulk density ρ_s or the void ratio ϵ of the sample in the unloaded condition, *i.e.* before the stresses σ and τ are applied. This density is called the initial bulk density. To simplify the representation of the diagram, conditions will be somewhat idealised. The curve traces drawn have the following meaning:

The curve f_1f_2 in the plane $\tau = 0$ is the line joining successive states of a loosely packed sample if stressed by an increasing compressive stress σ. This curve is called the "consolidation line".

The curve t_1t_2, also in the plane $\tau = 0$, represents the correlation between the void ratio and the tensile strength. States in the $\tau = 0$ plane outside these two lines are not possible.

In the tridimensional space two surfaces exist between these two curves. The intersection of these two surfaces is the curve e_1e_2. The surface between f_1f_2 and e_1e_2 is called the consolidation surface and the one between t_1t_2 and e_1e_2 the flow surface. This flow surface intersects the plane $\sigma = 0$ in the curve c_1c_2, thus giving the correlation between void ratio and cohesion. The curve e_1e_2 is called the "critical state line".

Both surfaces have the same significance as the yield surfaces in the principal stress space mentioned earlier: states below the surfaces are in elastic equilibrium, states on the surfaces cause a plastic deformation and states above the surface are not possible. The surfaces of this diagram are not yield surfaces as understood in plasticity theory, since the bulk density ρ_s or the void ratio ϵ are variables and not parameters as defined by plasticity theory.

Therefore the principle of normality [1] cannot be applied to this condition-diagram, to obtain the principal strain rates in the principal stress space.

The curve ACH is the "swelling curve", obtained when the compressive stress σ acting on a sample after consolidation to point A is reduced to $\sigma = 0$, thus representing the elastic recovery. The vertical wall above the swelling curve is the "elastic wall" and the intersection lines between these walls and both surfaces are called "elastic limit" curves. All of these labelling terms are taken from Roscoe. The "elastic limit" curves are connecting lines of states which yield to failure of samples of the same initial bulk density. Projecting these "elastic limit" curves on a plane ϵ = const., the lines I'L'E' and A'E' are obtained. The significance of these lines will be explained later.

With the aid of this condition-diagram it is possible to predict the behaviour of granular material in a known initial state when subjected to a given stress path or to given deformation conditions. In order to clarify the interpretation of this condition-diagram, three theoretical shear tests are performed and the successive states in this diagram are traced:

(1) A sample of void ratio ϵ_4 is stressed by a compressive stress σ_1 (point B) and is sheared. At constant void ratio the shear stress will increase up to point F, where the consolidation surface is reached. Since σ_1 is held constant, the void ratio ϵ will decrease whilst the shear stress is still increasing. This process stops at point E at the critical state line where the sample can continue to undergo extensive shear distortion without further changes of void ratio or stress.

(2) A sample of void ratio ϵ_1 is stressed by the same compressive stress σ_1 (point D) and is sheared. At point G the flow surface is reached and the material begins to dilate, *i.e.* the void ratio will increase and smaller shear stresses will be necessary to keep the material flowing. The critical state line is reached in E, where the dilated part of the sample is flowing under steady-state conditions.

(3) Starting with void ratio ϵ_2 and the same compressive stress σ_1 point C is obtained, which lies directly below the critical state line. In the shear process the shear stress is increasing up to a constant maximum value without volume change.

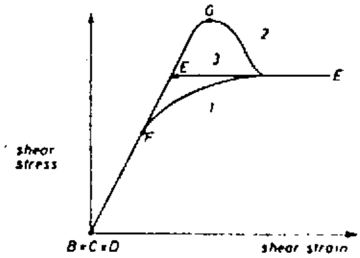

Fig. 3. Shear stress *vs.* shear strain graph with the three examples as shown in Fig. 2.

In a shear stress *versus* shear strain graph the curve traces of the three examples are as follows (Fig. 3): In the first test, starting at point B, we have a linear rise up to point F and then a smaller rise up to the line EE. In the second example the linear rise continues to point G and the line then falls to EE. In the third test a nearly linear rise up to the line EE is obtained.

It is evident that the critical state line divides the states of a material into two regions: firstly "looser than critical" or underconsolidated, which includes all states below the consolidation surface, and secondly "denser than critical" or overconsolidated, which includes all states below the flow surface. So long as the compressive stress is positive, the critical state line can be reached resulting in steady-state flow in at least a small band of the sample.

The projected lines A'E' and I'L'E' of Fig. 2 can be identical with the yield locus and the consolidation locus as measured in shear tests [2]. If the states of stress on samples of the same initial bulk density which lead to plastic flow are represented in the form of Mohr circles for stress in a τ, σ diagram (Fig. 4), the envelopes to these circles represent the yield condition. The left part is called the yield locus, where plastic flow results in an increase in volume, whereas the right part, called the consolidation locus, will lead to a decrease in volume. At the transition between these loci, steady-state flow without volume change will be obtained. Three possible transitions of the yield locus into the consolidation locus are represented in Fig. 4. The following discussion shows which of the three possibilities are realistic and agree with the condition-diagram and the definition of yield conditions.

(a) In Fig. 4(a) there is no smooth transition

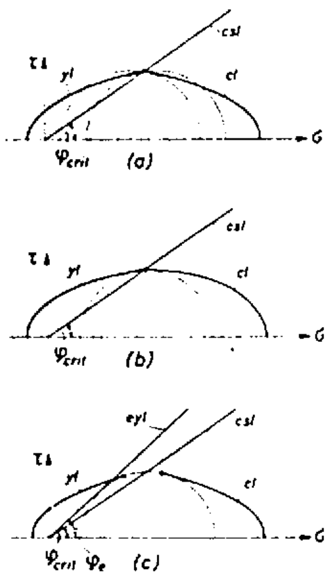

Fig. 4. Possible transitions of the yield locus into the consolidation locus. yl = yield locus, cl = consolidation locus, csl = critical state line.

between the two loci. This representation is compatible with the condition-diagram, but not with the definition for yield conditions, for the following reasons. At the transition point two Mohr circles are possible, one tangential to the yield locus and the other tangential to the consolidation locus. Both cross either the consolidation locus or the yield locus. The definition of the yield condition does not permit states outside these curves, *i.e.* this representation is physically not acceptable.

(b) A smooth transition with a horizontal tangent as shown in Fig. 4(b) is compatible with the condition-diagram and the definition of the yield condition.

(c) The third possibility is shown in Fig. 4(c). Here the two loci have different end-points. At these points the inclinations of the tangents are greater than zero or less than zero. The end-points are not identical as in the cases (a) and (b), but belong to the same Mohr circle for stress representing the steady-state flow. This figure is compatible with the definition for yield conditions, but not with the condition-diagram. The part of the Mohr circle between the two end-points completes the representation of the yield condition in this area of the τ, σ graph. In the condition-diagram (Fig. 2), only one state-point represents this condition.

Assuming this figure to be correct, the projected lines A′E′ and E′L′I′ in the condition-diagram are not identical with the yield locus and the consolidation locus. In the condition-diagram they are the connecting lines of the stress points (σ,τ), as measured in shear tests at incipient plastic flow.

Assuming isotropic behaviour in a shear test, the measured shear and compressive stresses at steady-state flow correspond to the vertex point of the equivalent Mohr circle for stress. Thus the critical state lines of Fig. 4(b) and (c) are identical. Roscoe does not discuss the question of possible transitions of the yield locus into the consolidation locus. Reading his published papers, one can suppose that he thinks of case (b) as correct.

The question of possible transitions does not arise in Jenike's papers, since he is interested only in overconsolidated yield loci. To characterise the steady-state flow he introduced an effective yield locus which is the envelope to the Mohr circles of steady-state flow for different bulk densities, *i.e.* for different yield loci. The use of this effective yield locus, which is generally a straight line through the origin inclined at angle φ_e against the abscissa, has mathematical advantages. In Jenike's papers the inclination of yield loci at their end-points is always greater than zero thus according to Fig. 4(c).

Case (a) is physically not acceptable, and most tests on granular materials carried out in powder technology show a behaviour which is more in accordance with case (c) than with case (b). Therefore case (c) will be assumed to be representative. Experiments must show if case (b) is at all possible in powder technology.

SHEAR TESTS

Before describing the shear behaviour in common shear apparatuses one should consider which shear tests are possible. Figure 5 shows the two extreme cases. "a" is the case of pure coulomb friction without volume change. The other extreme is a shear process ("b"), where the shearing takes place homogeneously throughout the sample. Volume changes occurring in most cases of the flow of granular materials are possible. Most of the available shear apparatuses behave neither as in case (a) nor as in case (b). The shear process

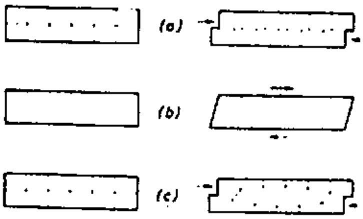

Fig. 5. Shear tests.

in the flow-factor tester of Jenike is shown for comparison in (c). Inside the lense-shaped shearing zone case (b) is nearly realised; outside this zone the material is moving as in case (a).

At the Institute of Mechanical Process Engineering at the University of Karlsruhe we have run tests with the tester of Jenike and another shear apparatus called a simple shear apparatus, in which the shear process of case (b) is approximately realised. Before reporting on the results, some comments must be made on the interpretation of shear test results.

In shear tests of the three cases shown in Fig. 5, the horizontal direction is for design reasons a direction without strain, *i.e.* the strain rate $\dot{\epsilon}_h = 0$. In tests without volume change as in the end-point of a yield locus the vertical strain is also zero ($\dot{\epsilon}_v = 0$). Thus the centre of the Mohr circle for strain rate with $\dot{\epsilon}$ as normal strain rate and $\dot{\gamma}/2$ as angular strain rate is in the origin of the $\dot{\epsilon}$, $\dot{\gamma}/2$ graph (Fig. 6a). The angle between the vertical and the direction of major principal strain rate $\dot{\epsilon}_1$ is $\pi/2$ in the Mohr circle, *i.e.* $\pi/4$ in the shear test. If isotropy is assumed, the directions of

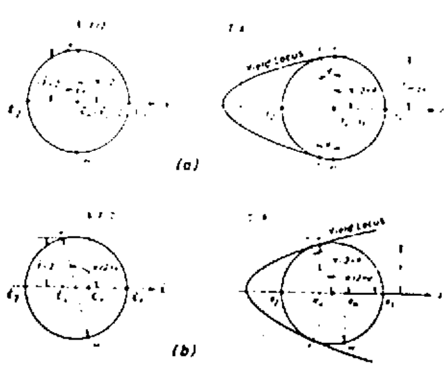

Fig. 6. Mohr circles for strain rate and stress for shear tests without volume change (a) and with volume increase (b).

principal stress σ_1 and principal strain rate $\dot{\epsilon}_1$ must coincide and σ_1 must act in a direction inclined at $\pi/4$ to the vertical. Therefore the stresses σ and τ acting in a horizontal plane are represented by point V in the Mohr circle for stress (Fig. 6a) as the vertex of the circle. As can be seen, point V is not identical with the tangential point T to the yield locus giving the direction of the slip planes in relation to the principal stress planes.

In tests yielding further points of a yield locus on the left of its end-point, an increase in volume is observed: $\dot{\epsilon}_1 + \dot{\epsilon}_2 < 0$. Since there is no horizontal strain, the vertical strain rate must become $\dot{\epsilon}_v < 0$, and the Mohr circle for strain rate is obtained, represented in Fig. 6(b). In this case the angle between the vertical and the direction of $\dot{\epsilon}_1$ is $\pi/4 + \nu/2$. The value of ν can only be obtained if the vertical strain rate $\dot{\epsilon}_v$ and the angular strain rate $\dot{\gamma}/2$ are measured. The equivalent Mohr circle for stress is also shown in Fig. 6(b). As in Fig. 6(a), points T and V are not identical.

If the material behaves isotropically, being one of the assumptions in the theory of Jenike, the horizontal shear plane, which in most apparatuses is forced upon the sample, is not identical with a slip plane. Knowing the angle φ one can predict the directions of the slip planes in relation to each other and to the direction of principal stresses. In metals, where the yield locus is parallel to the σ-axis, points V and T coincide ($\varphi = \nu = 0$), and the two slip planes intersect at an angle of $\pi/2$. In the flow of bulk solids this angle is different from $\pi/2$, as can be seen *e.g.* from the theory of Jenike and from the experimental results of Cutress, who used X-rays [17]. Thus $\varphi \neq \nu$ and points T and V cannot coincide.

In the flow-factor tester of Jenike [13 - 16] and in ring shear cells [18 - 20] the normal compressive stress σ and the shear stress τ in the horizontal shear plane are measured, thus resulting in point V. Since in Jenike's tester the angular strain rate $\dot{\gamma}/2$ and normal strain rate $\dot{\epsilon}$ cannot be determined, a value for ν cannot be obtained and it is not possible to draw a complete Mohr circle without a further assumption. Jenike assumed that in shear tests for yield points to the left of the end-point of yield loci the horizontal plane is a slip plane (T = V in Fig. 6b), and in tests yielding an end-point the horizontal is neither a slip plane (T = V in Fig. 6a) nor a plane of maximum shear stress (point V in Fig. 6a), but lies between these two possibilities. This is in disagreement with the assumption of isotropy. So one aim of our investigations was to run shear tests where the complete state of stress can be measured in order to see if the real behaviour agrees with Jenike's assumption or with the assumption of isotropy.

We performed our experiments with limestone of particle size $< 15\ \mu m$. In a first approach all test results with Jenike's tester were evaluated using the assumption of Jenike, *i.e.* letting the horizontal plane be identical with slip planes with the exception of the tests leading to end-points of yield loci.

As mentioned previously, one of the disadvantages of the Jenike tester is that a horizontal shear direction is forced upon the sample, and that the horizontal plane is assumed to be identical with a slip plane in the material at the maximum value of the shear force. During the shear process the direction of the major principal stress has to be rotated from the vertical from $\delta = 0$ at $\tau = 0$ to $\delta = \pi/4 + \varphi/2$ (see Fig. 6; for point T : $2\delta = \pi/2 + \varphi$). Whether this occurs or not, cannot be proved.

A shear apparatus in which the state of stress can be determined completely is the simple shear apparatus of Roscoe [3,9,10]. Since it was designed to meet the demands of soil mechanics, some changes had to be made to make the apparatus effective for use in powder technology.

Figure 7 shows a schematic drawing of the simple shear apparatus as existing in the Institute of Mechanical Process Engineering at the University of Karlsruhe [2,21,22]. The sample of 10 by 10 cm^2 and about 2 cm high is stressed by a vertically guided plunger with a normal force N. On the bottom of the apparatus a shear force S is acting. This shear stress is uniformly transmitted layer by layer from the bottom to the top of the sample. Both side planes, which are vertical before the application of the shear force S, can be rotated about the points a and can move in the slits b. Thus the sample can be deformed in the same way as it would be without boundaries, if the same shear stress is acting on each element of the sample. A vertical strain and a change in the shear angle α can be read from the micrometers c and d. For measuring the stresses, special load cells 1 - 8 with electric strain gauges have been developed. The state of stress in the inner third of the sample is needed for calculation purposes. To draw the stress Mohr circle, the stresses on the planes between f and g and h and i are determined from the stress readings of the load cells 1, 4 and 7 and 3, 6 and 8 respectively. Thus Mohr circles for stress and strain can be obtained completely and independently. It is outside the scope of this paper to describe the simple shear apparatus in detail, to explain the difficulties and necessary care in running tests and to report on the method of evaluating test results (for more details see [2]).

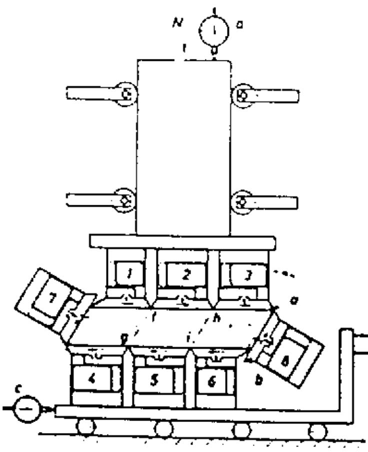

Fig. 7. Simple shear apparatus.

RESULTS AND DISCUSSION

In the next three figures some of the results are shown which give an answer to the question put forward in this paper. In Fig. 8 the angle δ between the vertical and the direction of the

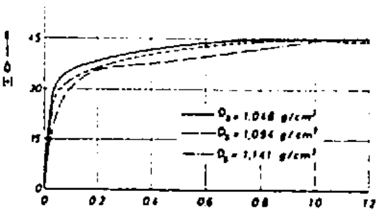

Fig. 8. Angle δ between the vertical and the direction of major principal stress *vs.* shear angle α for tests without volume change.

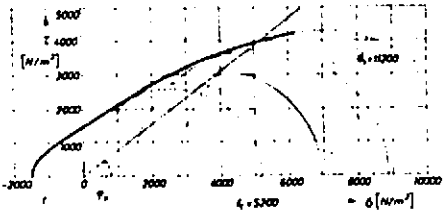

Fig. 9. Yield locus from tests with the simple shear apparatus (initial bulk density $\rho_s = 1.048$ g/cm^3).

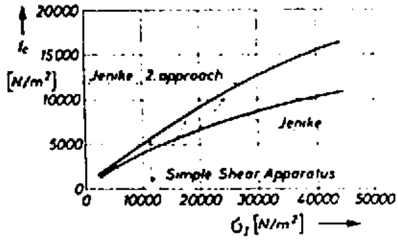

Fig. 10. Unconfined yield strength f_c vs. major principal stress at steady-state flow σ_1.

major principal stress is plotted against the shear angle α. The three curves are results from tests on samples with different bulk densities ρ_s leading to end-points of yield loci without volume change. In all three cases a constant maximum angle of $\delta = \pi/4$ is reached, which is in accordance with the assumption of isotropy. In tests yielding further points on the yield loci, the angle δ is greater than $\pi/4$ but smaller than $\pi/4 + \varphi/2$, thus showing the behaviour predicted in Fig. 5. It is noteworthy that only a shear angle of about 1° is necessary to reach the condition of steady-state flow.

Drawing the greatest Mohr circles for stress of tests on samples with the same initial bulk density in a τ,σ graph, a yield locus is obtained as the envelope to these circles. Such a yield locus is shown in Fig. 9. The tensile strength t as the minor principal stress of the smallest Mohr circle is determined in special tensile strength measurements [2]. By plotting a circle through the origin tangential to the yield locus the unconfined yield strength f_c is obtained, which, together with the major principal stress σ_1 of the Mohr circle through the end-point of the yield locus, gives one point on the failure function $f_c(\sigma_1)$, which is a characteristic function of a granular material and which is needed, for example, for the design of bins and hoppers.

Figure 10 shows the failure function obtained from a series of tests in which a family of yield loci was obtained, using a Jenike tester. The unconfined yield strength f_c is plotted as a function of the major principal stress σ_1 at steady-state flow. The curve labelled Jenike is obtained by using Jenike's assumptions, which is called the first approach (Table 1). If the same test results are taken, but — contrary to the first approach — isotropic behaviour in the shear test is assumed, the measured values of τ and σ will give the vertex points of the Mohr circles for tests leading to end-points of yield loci. By simplifying the procedure in assuming the same for all tests in a second approach ($\nu = 0$ in Fig. 6b), all Mohr circles can be drawn in the same way and yield loci are obtained as envelopes to these circles. Since these yield loci have greater τ-values, f_c will also be greater and the curve called "Jenike 2nd approach" must be

TABLE 1

Evaluation of shear test results

	No volume change (end-point of yield locus) (see also Fig. 6a and b)	Volume increase (left of end-point)
Jenike 1st approach	$T \neq V$ $\pi/4 < \delta < \pi/4 + \varphi/2$	$T = V$ $\delta = \pi/4 + \varphi/2$
Jenike 2nd approach	$T \neq V$ $\delta = \pi/4$	$T \neq V$ $\nu = 0$ $\delta = \pi/4$
Simple shear apparatus	$\delta = \pi/4$ $\pi/4 \leq \delta < \pi/4 + \varphi/2$ $\varphi > \nu \geq 0$	$\delta = \pi/4 + \nu/2$

loacted above the first approach curve. On the same graph (Fig. 10), three values obtained from tests with the simple shear apparatus are plotted. These points lie above the first Jenike curve, as is to be expected, but below the second Jenike curve. This can be explained by the fact that in the second approach δ is assumed to be $\delta = \pi/4$ for all cases. However, the tests in the simple shear apparatus show that $\pi/4 \leq \delta < (\pi/4 + \varphi/2)$, thus resulting in $\varphi > \nu \geq 0$. It thus appears that the first method of using the Jenike tester results underestimates the unconfined yield strength and the second approach overestimates f_c.

In each test with Jenike's shear tester or with the ring shear cells, only one pair of values of shear and compressive stress is measured and not the complete state of stress in the form of a Mohr circle for stress. The exact positions of the yield loci and therefore of the function $f_c\ (\sigma_1)$ can only be obtained if the deformation of the sample is homogeneous and all strain rates are measured. With these measured strain rates the Mohr strain rate circle can be drawn and the angle ν can be read from the graph. With the knowledge of this angle and the proven behaviour of isotropy, the Mohr stress circle can be obtained. This procedure is never possible with Jenike's tester, since the thickness and the shape of the zone where the shearing takes place are unknown. In principle it should be possible to run a shear test in a ring shear cell with homogeneous deformation up to the point of yield. But in any case the homogeneity of deformation has to be confirmed, for example by using γ-rays. It follows from the results with the simple shear apparatus amongst others that the tangent to the end-point of a yield locus has a positive inclination greater than zero (Fig. 9). Referring back to Fig. 4, the behavior predicted by case (c) for the tested material seems to be correct. More research is necessary to get a better idea of what happens in this area, especially in the position and the end-point of the consolidation locus. To my knowledge no papers have been published reporting on measurements of consolidation loci of granular materials in powder technology.

CONCLUSIONS

The investigations have shown that:

(1) Granular materials show isotropic behaviour up to the point where the state of flow is reached.

(2) The horizontal plane in a shear test is not identical with a slip plane.

(3) Only small shear angles of less than 1° are necessary to reach the state of flow. In Roscoe's experiments with a coarse cohesionless sand shear angles of 10° and greater were measured [9,10].

(4) Tests with Jenike's flow-factor tester give similar results to those with the sample shear apparatus, if properly interpreted.

REFERENCES

1 R. Hill, The Mathematical Theory of Plasticity, Oxford Univ. Press, London, 1960.
2 J. Schwedes, Scherverhalten leicht verdichteter, kohäsiver Schüttgüter, Diss., Univ. Karlsruhe, 1971.
3 K.H. Roscoe, An apparatus for the application of simple shear to soil samples, Proc. 3rd Int. Conf. Soil Mech., 1 (1953) 186 - 191.
4 K.H. Roscoe, A.N. Schofield and C.P. Wroth, On the yielding of soils, Geotechnique, 8 (1958) 22 - 53.
5 K.H. Roscoe, A.N. Schofield and A. Thurairajah, An evaluation of test data for selecting a yield criterion for soils, Symp. Laboratory Shear Testing of Soils, Ottawa, 1963, pp. 111 - 133.
6 K.H. Roscoe, A.N. Schofield and A. Thurairajah, Yielding of clays in states wetter than critical, Geotechnique, 13 (1963) 211 - 240.
7 K.H. Roscoe and A. Thurairajah, On the uniqueness of yield surfaces for wet clays, in Rheology and Soil Mechanics, Springer, Berlin, 1966, pp. 364 - 381.
8 C.P. Wroth and R.H. Basset, A stress - strain relationship for the shearing behaviour of a sand, Geotechnique, 15 (1965) 32 - 56.
9 K.H. Roscoe, R.H. Basset and E.R.L. Cole, Principal axes observed during simple shear of sand, Proc. Conf. on Shear strength properties of natural soils and rocks, Oslo, 1967, 1, pp. 231 - 237.
10 K.H. Roscoe, Discussion in Proc. Conf. on Shear strength properties of natural soils and rocks, Oslo, 1967, 2, pp. 188 - 192.
11 K.H. Roscoe and J.B. Burland, On the generalized stress-strain behaviour of "wet" clay, in Engineering Plasticity, Cambridge Univ. Press, Cambridge, 1968, pp. 535 - 609.
12 K.H. Roscoe, The influence of strains in soil mechanics, Geotechnique, 20 (1970) 129 - 170.
13 A.W. Jenike, Gravity flow of bulk solids, Bull. 108, Eng. Expt. Sta., Utah State Univ., 1961.
14 A.W. Jenike, Gravity flow of solids, Trans. Inst. Chem. Engrs., 40 (1962) 264 - 271.
15 A.W. Jenike, Storage and flow of solids, Bull. 123, Eng. Expt. Sta., Utah State Univ., 1964.
16 A.W. Jenike, P.J. Elsey and R.H. Woolley, Flow properties of bulk solids, Proc. Amer. Soc. Test. Mater., 60 (1960) 1168 - 1190.

17 J.O. Cutress and R.F. Pulver, X-ray investigations of flowing powders, Powder Technol., 1 (1967) 207 - 212.

18 J.F. Carr and D.M. Walker, An annular shear cell for granular materials, Powder Technol., 1 (1967/68) 369 - 373.

19 B. Scarlett and A.C. Todd, A split ring annular shear cell for the determination of the shear strength of a powder, J. Sci. Instr., Ser. 2, 1 (1968) 655 - 656.

20 E. Goldacker, Untersuchungen zur inneren Reibung von Pulvern, insbesondere im Hinblick auf die Förderung in Extrudern, Diss., TH Aachen, 1971.

21 J. Schwedes, Bestimmung der Schüttguteigenschaften zur Dimensionierung von Bunkern, Chem. Ingr.-Tech., 44 (1972) 400 - 404.

22 J. Schwedes, Measurement of powder properties for hopper design, Trans. ASME, J. Eng. Ind., Ser. B., 95 (1) (1973) 55 - 59.

American Society of Mechanical Engineers. Journal of Engineering for Industry